EUROPEAN JOURNAL OF COMPUTATIONAL MECHANICS, 2017
VOL. 26, NOS. 5–6, 541–556
https://doi.org/10.1080/17797179.2017.1382317

Taylor & Francis
Taylor & Francis Group

An FEM-based AI approach to model parameter identification for low vibration modes of wind turbine composite rotor blades

N. Navadeh[a], I. O. Goroshko[b], Y. A. Zhuk[b] and A. S. Fallah[a]

[a]Department of Aeronautics, South Kensington Campus, Imperial College London, London, UK; [b]Department of Theoretical and Applied Mechanics, Taras Shevchenko National University of Kyiv, Kiev, Ukraine

ABSTRACT

An approach to construction of a beam-type simplified model of a horizontal axis wind turbine composite blade based on the finite element method is proposed. The model allows effective and accurate description of low vibration bending modes taking into account the effects of coupling between flapwise and lead–lag modes of vibration transpiring due to the non-uniform distribution of twist angle in the blade geometry along its length. The identification of model parameters is carried out on the basis of modal data obtained by more detailed finite element simulations and subsequent adoption of the 'DIRECT' optimisation algorithm. Stable identification results were obtained using absolute deviations in frequencies and in modal displacements in the objective function and additional a priori information (boundedness and monotony) on the solution properties.

ARTICLE HISTORY
Received 7 June 2017
Accepted 18 September 2017

KEYWORDS
Low-dimensional beam model; AI; optimisation algorithm; vibration coupling; flapwise vibration; lead–lag mode

1. Introduction

The main tendency, throughout the past decades, in the evolution of wind energy technology has been the growth in size of wind turbines. This is attributed to both economic and technological reasons since employing larger turbines leads to enhancing performance and increased capacity of production in wind energy projects (Serrano-González & Lacal-Arántegui, 2016; Wiser & Bolinger, 2015). However, scaling up wind power plants gives rise to new challenging problems in the design and operation of single turbines as well as wind farm spacing and turbine poising, the solution to which requires versatile tools. As far as a single turbine is concerned an increase in the length of the blade necessitates more intensive investigations in structural dynamics performance of the blade and re-evaluation of stresses evolved. In particular, serious issues arise due to adoption

CONTACT A. S. Fallah as3@imperial.ac.uk

of long slender blades for modern wind turbines, which are much more flexible than earlier ones. The possible intense vibrations in service conditions can not only cause fatigue damage or affect structural strength and stability, but also have significant influence on power production (Staino & Basu, 2015).

In the past, wood and aluminium were used in construction of blades but nowadays wind turbine blades are almost universally made of composite materials with wooden stiffeners as secondary structural elements. This allows reducing their weight through attaining higher stiffness-to-weight and strength-to-weight ratios. The question of simultaneous optimal design of composite blades to achieve both aerodynamic efficiency and structural strength are considered in Chen and Chen (2010). The resulting design for the blade yields a composite shell structure, as the primary load bearing element, encompassing standard NREL airfoil sections, rather inhomogeneous (slenderised towards the end) and structurally pre-twisted along its length.

Finite element methods (FEMs), as realised in modern commercial CAE packages (ANSYS, ABAQUS, NASTRAN, etc.), form a strong suite for simulation of static and dynamic response of structural and mechanical systems with high accuracy. The element libraries of these pieces of software are comprehensive and include 1D, 2D and 3D elements. Furthermore, the software allows use of doubly curved shell elements with composite through-thickness lay-ups. The analyses conducted here are on the basis of homogenised anisotropic shell elements for model representation, using not too much of computer resources. But in many cases, e.g. investigation of general structural dynamics, aero-elastic vibrations, or preliminary design of vibration control in mechanical and aerospace systems, such detailed models are superfluous and can be replaced by simplified beam type models which allow to describe general blade deformations with appropriate accuracy and require much less simulation time and computational resources. The same scenario is encountered when setting up models for different slender aerospace structures: in many cases wings, fuselages, etc. can be considered using simplified one-dimensional beam and rod approximations.

Several approaches to obtaining a simplified model exist. One group of methods utilises direct approximation techniques based on energy equivalence, method of virtual displacements or minimum total potential energy (Lee, 1995). An alternative group consists of methods employing parameter identification techniques applying various optimisation methods or methods of Artificial Intelligence such as Artificial Neural Networks (ANN's) to obtain models whose results are best fitted (in the sense of selected measurable outcomes) to data, obtained from physical experiments or computer simulations, using more precise but more resource-consuming and computationally immoderate models (Trivailo, Dulikravich, Sgarioto, & Gilbert, 2006). Both types of methods work well for simple homogeneous and weakly inhomogeneous structures, but in more complicated cases parameter identification has definite advantages. Also, these approaches can be combined, so that identification is used to correct parameters of models derived

by direct methods. In the latter, the form of the model is fixed and parameters are adjusted so that the model represents certain behaviour faithfully.

Traditionally, it is known that parameter identification is an ill-posed problem, and in general there are issues with instability and non-uniqueness of solution. The effectiveness and quality of parameter identification largely depends on the structure and size of a chosen mathematical model, on appropriate selection of identified parameters, and on objective function(s) which describes and quantifies the error between model prediction and experimental data (or the ANN configuration and settings, when it is used). In dealing with such ill-posed problems, it is very useful to take into account additional a priori information about solution properties, e.g. the limitedness and monotonicity (Bakushinsky & Goncharsky, 1994).

In the present paper, modal analysis of a horizontal axis wind turbine (HAWT) composite blade is conducted using the finite element technique. Then a simplified model is proposed which consists of discrete masses connected by one-dimensional beam segments. In this low-dimensional beam model representing the fundamental vibration modes of the blade, the real blade is approximated by a piecewise homogeneous cantilever beam consisting of several sections with lumped masses located at the connection points between sections and at the end point. In order to take account for blade pre-twisting in the framework of the model developed, for each piecewise homogeneous beam section, the principal axes are chosen to be oriented along local coordinate axes, which are rotated by some angle around the beam axis. Then, by making use of Euler–Bernoulli beam theory and presenting general solutions of beam equations as third order polynomials as well as continuity conditions between the beam segments and at the end points, the problem is reduced to the system of differential-algebraic equations with constant coefficients which describe free vibrations of the considered beam-mass model. The natural frequencies and vibration modes for a generically considered segmented beam can be easily determined. The physical parameters of the approximate beam-mass model developed are then identified with the application of an effective global minimisation procedure through extensive use of modal information obtained by FEM simulations.

2. Finite element analysis of blade vibration

In order to propose a simplified low-dimensional beam-type model of a wind turbine blade, we need to have sufficiently precise information on the dynamic properties of the investigated object. In the present case, as a source of reference data, we use the results of finite element simulations based on the three-dimensional model of turbine blade. This model is set up in the commercial FEM package ABAQUS (2014) employing shell elements for the representation of the structure. The geometry of the blade is based on the results of optimised blade design obtained in Chen and Chen (2010) (except that internal stiffeners were

omitted). Material of the blade is supposed to be unidirectional composite with fibres predominantly aligned along its length. The laminated fibre-reinforced composite shell is homogenised through the thickness so that an anisotropic shell of equivalent thickness is obtained. Details of non-structural parts are not included as they only contribute to unnecessary sophistication of the model. The blade model consists of five sections with different wall thicknesses. Figure 1 shows the general blade FEM model structure.

Section wall thicknesses and material constitutive parameters are given in Tables 1 and 2.

Modal computations conducted in ABAQUS provide a series of the natural frequencies for the turbine blade. The six lowest frequencies which correspond to bending vibrations of the blade are presented in Table 3. It is worth mentioning here that because of structural pre-twisting, the blade hasn't pure flap and lead-lag vibrations indeed. They are coupled here but flap vibrations prevail.

Corresponding modal displacements were extracted in the nodes along the top and bottom reference lines in the blade FEM model. The results are presented in Figure 2, where the upper graphs show flap displacements $v = u_y$, and lower graphs show lead–lag displacements $u = u_x$.

3. Low-dimensional beam model of turbine blade

In order to build a low-dimensional beam model representing the fundamental vibration modes of the blade, the real blade is approximated by a piecewise homogeneous cantilever beam consisting of N sections of length L_k with lumped masses $m_k, k = \overline{1, N}$, located at the connection points between sections and at the end point (see Figure 3). As depicted the z-axis is oriented along the beam, while the y-axis is in the flap direction and the x-axis is in lead-lag bending direction. Here, we use the Euler–Bernoulli beam model because the blade is long and slender in y direction and the vibration in this direction is considered mainly, while for the lead-lag x motions, the lower modes of interest can be considered using long-wave approximation.

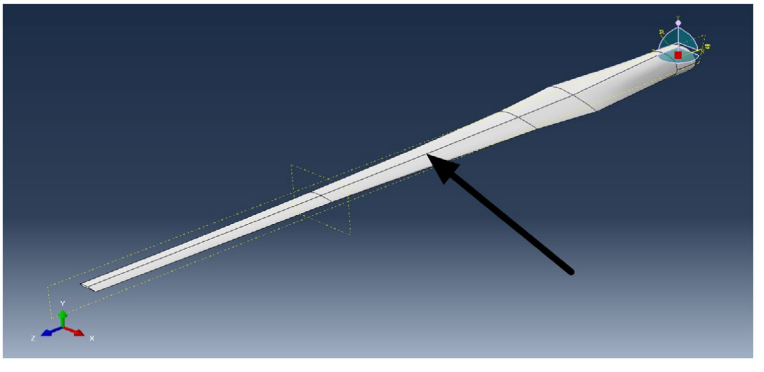

Figure 1. FEM model geometry of composite wind turbine blade.

Table 1. Section thicknesses along the beam axis (measured from the circular root).

Distance from the root z (mm)	Thickness t (mm)
1754	96.02
9648	79.04
14,251	53.21
29,212	13.44
44,175	10.34

Table 2. Stiffness moduli and Poisson ratios for the UD composite (1 – direction of fibre, 2 – transverse direction 3 – direction through the thickness).

ρ (kg/m^3)	E_1 (MPa)	E_2 (MPa)	E_3 (MPa)	ν_{12}	ν_{13}	ν_{23}	G_{12} (MPa)	G_{13} (MPa)	G_{23} (MPa)
1860	3.7×10^{10}	1.80×10^{10}	1.80×10^{10}	.25	.25	.3	8×10^9	8×10^9	6.9×10^9

Table 3. Computed natural frequencies for wind turbine blade.

Mode number	1	2	3	4	5	6
Frequency (Hz)	.52	1.81	2.33	4.07	6.37	7.27

The analysis of the graphs for modal displacements obtained by ABAQUS simulations on the model presented in Figure 2 shows rather strong coupling between flap and lead-lag motions for the second and third modes due to the twisting of the structure along its length. This leads to the conclusion that the simple model possessing few degrees-of-freedom (beams-and- lumped masses model of Figure 3) should contain a mechanism to describe this effect. Also, we can note that torsion is not considerable for the six low modes, and in the sequel will be neglected.

Thus, to take into account the blade twisting, we build the model where each k-th piecewise homogeneous beam section, the principal axes of which are oriented along local coordinate axes, are rotated by the angle α_k around the z-axis (Figure 4).

In local coordinates, for the k-th homogeneous weightless section, the beam deformation is described by standard Euler–Bernoulli beam equations:

$$(EI_y)_k \frac{\partial^4 u_k}{\partial z^4} = 0 \quad \text{and} \quad (EI_x)_k \frac{\partial^4 v_k}{\partial z^4} = 0, \tag{1}$$

where $(EI_y)_k$ and $(EI_x)_k$ are bending stiffnesses. Since in our case the beam sections are connected to masses and are parts of the dynamic system, displacement components depend not only on z coordinate, but also on time t: $u_k = u_k(z, t)$, $v_k = v_k(z, t)$. It must, however, be noted that distributed beam masses are not considered and only the lump masses are. In other words, as far as system stiffness is concerned we are dealing with a distributed stiffness of a continuous system, whereas for the dynamic analyses the masses are concentrated and we are dealing with a discrete parameter model.

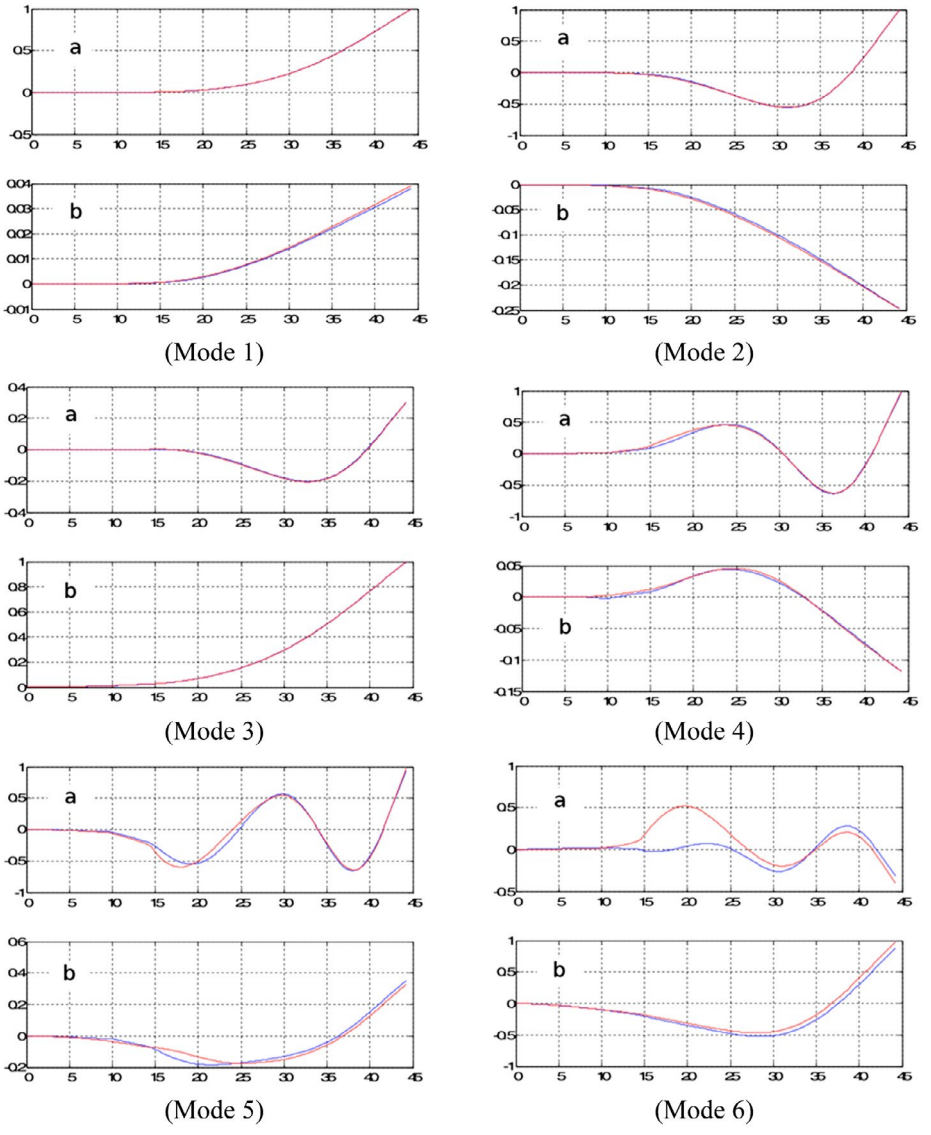

Figure 2. Computed modal displacements: (a) in the *y* direction (flap), and (b) in the *x* direction (lead-lag).

Notes: Modes 1 – .5265 Hz, 2 – 1.8191 Hz, 3 – 2.332 Hz, 4 – 4.0737 Hz, 5 – 6.3726 Hz, 6 – 7.2776 Hz (blue and red lines correspond to the top and bottom reference lines in the blade FEM model).

General solutions of Equations (1) can be presented as polynomials of the third order. Using local coordinate ξ_k (measured from the beginning of the section in z direction), they can be written as:

$$u_k = a_0^{(k)} + a_1^{(k)}\xi_k + a_2^{(k)}\xi_k^2 + a_3^{(k)}\xi_k^3, \quad v_k = b_0^{(k)} + b_1^{(k)}\xi_k + b_2^{(k)}\xi_k^2 + b_3^{(k)}\xi_k^3. \quad (2)$$

As the generalised coordinated for the components of displacements, the coefficients $a_j^{(k)}$ and b_j^k in (2) are functions of time.

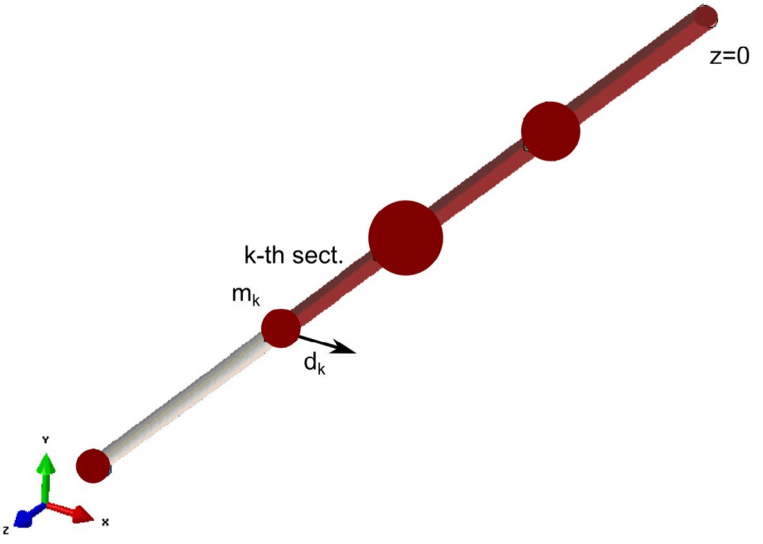

Figure 3. Structure of the beam-mass-simplified blade model.

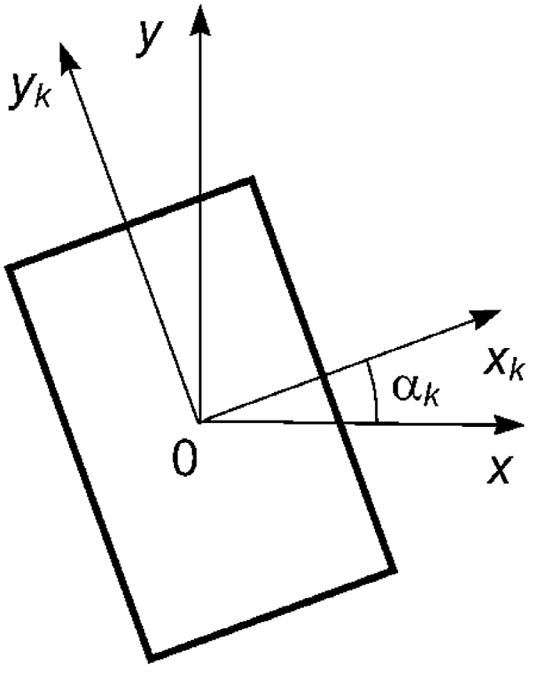

Figure 4. Orientation of the *k*-th homogeneous beam section corresponding to blade twisting.

The components of basis unit vectors of the *k*-th local coordinate system in the reference global coordinate system (subscript '0') are presented as:

$$\mathbf{e}_x^{(k)} = (\cos\alpha_k,\ \sin\alpha_k)_0, \quad \mathbf{e}_y^{(k)} = (-\sin\alpha_k,\ \cos\alpha_k)_0, \tag{3}$$

Thus, for the components of displacement vector for the k-th beam section, we have

$$\mathbf{u}_k = u_k \mathbf{e}_x^{(k)} + v_k \mathbf{e}_y^{(k)} = (u_k \cos\alpha_k - v_k \sin\alpha_k, \quad u_k \sin\alpha_k + v_k \cos\alpha_k)_0. \tag{4}$$

Of course, such transformations are universal and affect the components of any other vector, such as moments and forces.

Local components of bending moments thus take the form:

$$M_{xk} = -(EI_x)_k \frac{\partial^2 v_k}{\partial z^2}, \quad M_{yk} = (EI_y)_k \frac{\partial^2 u_k}{\partial z^2}. \tag{5}$$

And for shear forces we obtain:

$$Q_{yk} = \frac{\partial M_{xk}}{\partial z} = -(EI_x)_k \frac{\partial^3 v}{\partial z^3}, \quad Q_{xk} = -\frac{\partial M_{yk}}{\partial z} = -(EI_y)_k \frac{\partial^3 u}{\partial z^3}. \tag{6}$$

At the clamped point of the beam ($z = 0$), the cantilever beam essential boundary conditions hold which give for the coefficients of the beam solutions in Equation (2) $a_0^{(1)} = a_1^{(1)} = b_0^{(1)} = b_1^{(1)} = 0$. At the points of connection between sections continuity conditions must hold, i.e. the components, in the global coordinate system, of transversal displacements and their derivatives with respect to z as well as components of bending moments are continuous. It must be noted that and components of shear forces have jumps due to the inertial forces from the lumped masses. At the end free tip point, zero moment and shear force–inertial force conditions hold. These are the free-end natural boundary conditions.

Thus, the conditions of continuity between the first and the second beam sections give the following equations (hereinafter dots, as usual, denote temporal differentiation):

$$\begin{aligned}
&-(L_1^2 a_2^{(1)} + L_1^3 a_3^{(1)}) \cos\alpha_1 + a_0^{(2)} \cos\alpha_2 + (L_1^2 b_2^{(1)} + L_1^3 b_3^{(1)}) \sin\alpha_1 - b_0^{(2)} \sin\alpha_2 = 0,\\
&-(L_1^2 a_2^{(1)} + L_1^3 a_3^{(1)}) \sin\alpha_1 + a_0^{(2)} \sin\alpha_2 - (L_1^2 b_2^{(1)} + L_1^3 b_3^{(1)}) \cos\alpha_1 + b_0^{(2)} \cos\alpha_2 = 0,\\
&-(2L_1 a_2^{(1)} + 3L_1^2 a_3^{(1)}) \cos\alpha_1 + a_1^{(2)} \cos\alpha_2 + (2L_1 b_2^{(1)} + 3L_1^2 b_3^{(1)}) \sin\alpha_1 - b_1^{(2)} \sin\alpha_2 = 0,\\
&-(2L_1 a_2^{(1)} + 3L_1^2 a_3^{(1)}) \sin\alpha_1 + a_1^{(2)} \sin\alpha_2 - (2L_1 b_2^{(1)} + 3L_1^2 b_3^{(1)}) \cos\alpha_1 + b_1^{(2)} \cos\alpha_2 = 0,\\
&-(2a_2^{(1)} + 6L_1 a_3^{(1)})(EI_y)_1 \cos\alpha_1 + 2a_2^{(2)}(EI_y)_2 \cos\alpha_2 + (2b_2^{(1)} + 6L_1 b_3^{(1)})(EI_x)_1 \sin\alpha_1\\
&\quad -2b_2^{(2)}(EI_x)_2 \sin\alpha_2 = 0,\\
&(2a_2^{(1)} + 6L_1 a_3^{(1)})(EI_y)_1 \sin\alpha_1 - 2a_2^{(2)}(EI_y)_2 \sin\alpha_2 + (2b_2^{(1)} + 6L_1 b_3^{(1)})(EI_x)_1 \cos\alpha_1\\
&\quad -2b_2^{(2)}(EI_x)_2 \cos\alpha_2 = 0,\\
&6a_3^{(1)}(EI_y)_1 \cos\alpha_1 - 6a_3^{(2)}(EI_y)_2 \cos\alpha_2 - 6b_3^{(1)}(EI_x)_1 \sin\alpha_1 + 6b_3^{(2)}(EI_x)_2 \sin\alpha_2\\
&\quad = m_1(\ddot{a}_0^{(2)} \cos\alpha_2 - \ddot{b}_0^{(2)} \sin\alpha_2),\\
&6a_3^{(1)}(EI_y)_1 \sin\alpha_1 - 6a_3^{(2)}(EI_y)_2 \sin\alpha_2 + 6b_3^{(1)}(EI_x)_1 \cos\alpha_1 - 6b_3^{(2)}(EI_x)_2 \cos\alpha_2\\
&\quad = m_1(\ddot{a}_0^{(2)} \sin\alpha_2 + \ddot{b}_0^{(2)} \cos\alpha_2).
\end{aligned} \tag{7}$$

Then, from the conditions of continuity for connection points of other beam segments ($k = \overline{2, N-1}$), we obtain following equations:

$$
\begin{aligned}
&-(a_0^{(k)} + L_k a_1^{(k)} + L_k^2 a_2^{(k)} + L_k^3 a_3^{(k)}) \cos\alpha_k + a_0^{(k+1)} \cos\alpha_{k+1} \\
&\quad +(b_0^{(k)} + L_k b_1^{(k)} + L_k^2 b_2^{(k)} + L_k^3 b_3^{(k)}) \sin\alpha_k - b_0^{(k+1)} \sin\alpha_{k+1} = 0, \\
&-(a_0^{(k)} + L_k a_1^{(k)} + L_k^2 a_2^{(k)} + L_k^3 a_3^{(k)}) \sin\alpha_k + a_0^{(k+1)} \sin\alpha_{k+1} \\
&\quad -(b_0^{(k)} + L_k b_1^{(k)} + L_k^2 b_2^{(k)} + L_k^3 b_3^{(k)}) \cos\alpha_k + b_0^{(k+1)} \cos\alpha_{k+1} = 0, \\
&-(a_1^{(k)} + 2L_k a_2^{(k)} + 3L_k^2 a_3^{(k)}) \cos\alpha_k + a_1^{(k+1)} \cos\alpha_{k+1} \\
&\quad +(b_1^{(k)} + 2L_k b_2^{(k)} + 3L_k^2 b_3^{(k)}) \sin\alpha_k - b_1^{(k+1)} \sin\alpha_{k+1} = 0, \\
&-(a_1^{(k)} + 2L_k a_2^{(k)} + 3L_k^3 a_3^{(k)}) \sin\alpha_k + a_1^{(k+1)} \sin\alpha_{k+1} \\
&\quad -(b_1^{(k)} + 2L_k b_2^{(k)} + 3L_k^2 b_3^{(k)}) \cos\alpha_k + b_1^{(k+1)} \cos\alpha_{k+1} = 0, \\
&-(2a_2^{(k)} + 6L_k a_3^{(k)})(EI_y)_k \cos\alpha_k + 2a_2^{(k+1)}(EI_y)_{k+1} \cos\alpha_{k+1} \\
&\quad +(2b_2^{(k)} + 6L_k b_3^{(k)})(EI_x)_k \sin\alpha_k - 2b_2^{(k+1)}(EI_x)_{k+1} \sin\alpha_{k+1} = 0, \\
&(2a_2^{(k)} + 6L_k a_3^{(k)})(EI_y)_k \sin\alpha_1 - 2a_2^{(k+1)}(EI_y)_{k+1} \sin\alpha_{k+1} \\
&\quad +(2b_2^{(k)} + 6L_k b_3^{(k)})(EI_x)_k \cos\alpha_k - 2b_2^{(k+1)}(EI_x)_{k+1} \cos\alpha_{k+1} = 0, \\
&6a_3^{(k)}(EI_y)_k \cos\alpha_k - 6a_3^{(k+1)}(EI_y)_{k+1} \cos\alpha_{k+1} \\
&\quad -6b_3^{(k)}(EI_x)_k \sin\alpha_k + 6b_3^{(k+1)}(EI_x)_{k+1} \sin\alpha_{k+1} = m_k(\ddot{a}_0^{(k+1)} \cos\alpha_{k+1} - \ddot{b}_0^{(k+1)} \sin\alpha_{k+1}), \\
&6a_3^{(k)}(EI_y)_k \sin\alpha_k - 6a_3^{(k+1)}(EI_y)_{k+1} \sin\alpha_{k+1} \\
&\quad +6b_3^{(k)}(EI_x)_k \cos\alpha_k - 6b_3^{(k+1)}(EI_x)_{k+1} \cos\alpha_{k+1} = m_k(\ddot{a}_0^{(k+1)} \sin\alpha_{k+1} + \ddot{b}_0^{(k+1)} \cos\alpha_{k+1}).
\end{aligned}
\tag{8}
$$

And finally, moment and force conditions at the end point give:

$$
\begin{aligned}
&-(2a_2^{(N)} + 6L_N a_3^{(N)})(EI_y)_N \cos\alpha_N + (2b_2^{(N)} + 6L_N b_3^{(N)})(EI_x)_N \sin\alpha_N = 0, \\
&(2a_2^{(N)} + 6L_N a_3^{(N)})(EI_y)_N \sin\alpha_N + (2b_2^{(N)} + 6L_N b_3^{(N)})(EI_x)_N \cos\alpha_N = 0, \\
&6a_3^{(N)}(EI_y)_N \cos\alpha_N - 6b_3^{(N)}(EI_x)_N \sin\alpha_N = m_N \ddot{u}_{END}, \\
&6a_3^{(N)}(EI_y)_N \sin\alpha_N + 6b_3^{(N)}(EI_x)_N \cos\alpha_N = m_N \ddot{v}_{END}, \\
&(a_0^{(N)} + L_N a_1^{(N)} + L_N^2 a_2^{(N)} + L_N^3 a_3^{(N)}) \cos\alpha_N \\
&\quad -(b_0^{(N)} + L_N b_1^{(N)} + L_N^2 b_2^{(N)} + L_N^3 b_3^{(N)}) \sin\alpha_N - u_{END} = 0, \\
&(a_0^{(N)} + L_N a_1^{(N)} + L_N^2 a_2^{(N)} + L_N^3 a_3^{(N)}) \sin\alpha_N \\
&\quad +(b_0^{(N)} + L_N b_1^{(N)} + L_N^2 b_2^{(N)} + L_N^3 b_3^{(N)}) \cos\alpha_N - v_{END} = 0,
\end{aligned}
\tag{9}
$$

where u_{END} and v_{END} are displacement components of the tip in the global coordinate system.

The system of differential-algebraic equations with constant coefficients of Equations (7)–(9) describes free vibrations of the considered beam-mass model. These can be represented in compact matrix form as:

$$
Ac = B\ddot{c}, \tag{10}
$$

where $c = \left\{ \{a_j^k\}_{k=0}^N,\ \{b_j^k\}_{k=0}^N,\ u_{END},\ v_{END} \right\}$ and matrices A and B consist of coefficients in the left and right sides of Equations (7)–(9), respectively.

To find natural frequencies and vibration modes, the solution of Equation (10) is represented in the exponential form as follows:

$$c(t) = \bar{c}e^{\lambda t}. \tag{11}$$

Substitution from Equation (11) into Equation (10) leads to the generalised eigenvalue problem (Gruber, 2014) having the following form:

$$Ac = \lambda^2 Bc, \tag{12}$$

The solution of which gives the spectrum of eigenvalues, λ_k^2, and their corresponding eigenvectors, c_k. Then the natural cyclic frequencies of vibrations are calculated by the formulae $f_k = \sqrt{-\lambda_k^2}/(2\pi)$, and components of c_k are used to represent vibration modes of Equation (2).

On the basis of these relations, we developed a MATLAB function which computes natural frequencies and vibration modes for a generically considered N-section beam-mass models with coupling between vibrations in the x and y directions due to stepwise structural twisting.

4. Solving the parameter identification problem

The physical parameters of the approximate beam-mass model built in previous section need to be determined (identified) on the basis of known information on the behaviour of the real structure. In our case, we have data for bending vibrations of the composite wind turbine blade on lower natural frequencies and mode shapes, obtained earlier in section 2 by FEM simulations using ABAQUS. But it is known that using merely modal data one cannot provide a unique set of parameters of the system using the solution of the identification problem (Baruch, 1997). Because of this in the literature (see Trivailo et al., 2006) modal data were complemented by the values of beam bending stiffness, identified separately from static measurements, and subsequently modal data were used for determining model mass parameters.

Since we use, as the source of data on the reference structure, those data extracted from the FEM model with a well-defined geometry and known material density, it is more convenient to extract some data, such as the characteristics of mass distribution, from this model directly. Thus, for the five structural sections of the blade (see Table 1 and Figure 1), we obtain following mass distribution parameters shown in Table 4.

Table 4. Structural section masses and mass centre coordinates.

	Section mass (kg)	Mass centre coordinate (m)
1	2434.75	.877
2	8651.47	5.71
3	3150.87	11.85
4	1667.89	21.02
5	788.38	36.28

It should be noted that this structure segmentation is not tuned well enough for direct use in building a simplified model, as the most slender and flexible part of the blade which occupies two thirds of its length, is divided only into two parts (4 and 5), while the rest more rigid and less deformable root part is divided into three parts. Such structure of the model leads to inefficient accuracy in its approximation capability, as well as reduction in the stability of its solution.

Instead of following this discretisation, it is proposed to divide each of the long flexible parts 4 and 5 into two model parts, while combining the most rigid root parts 1 and 2 into one model part. In dividing the segments into finer parts, we have assumed a linear mass distribution on each segment, so masses of the obtained parts and coordinates of their mass centres can be easily calculated. Then transition from distributed to lumped masses was made using the 'principle of the lever', when after the replacement mass centre of each approximating model segment remains at its initial position.

For the considered case of the six segment beam-mass model we obtain following values of lumped masses at the nodes (kg): $m_1 = 6985.084$, $m_2 = 2003.617$, $m_3 = 833.945$, $m_4 = 556.534$, $m_5 = 394.19$, $m_6 = 175.308$.

Values of initial twisting angles α_k for homogeneous beam sections are estimated at their middle points on the basis of turbine blade twisting angle distribution given in (Chen & Chen, 2010), and assuming linear variation of twisting along the blade structural subsections. Obtained in such a way values of α_k (degrees) are as following: [−12.856, −10.263, −6.335, −3.665, −2.060, −1.520].

In order to solve the identification problem, we apply the effective global minimisation procedure using the DIRECT algorithm (DIRECT, 2003). The optimisation problem is formulated so that it determines the values of bending stiffnesses $(EI_x)_k$ and $(EI_y)_k$ which minimise the objective function (13) within constraints, i.e. lower and upper bounds for stiffness values and, in addition, the condition of decreasing bending stiffnesses from the root to end.

Extensive numerical experiments have shown that much better identification results are obtained when absolute deviations of frequencies and displacements are used instead of their squares in the objective function. Thus, the objective function which was used in the present study has following form:

$$F = q \sum_{m=1}^{N_f} \left| \frac{f_m}{f_m^{ref}} - 1 \right| + \sum_{k-1}^{N_d} \left(\int_0^{z_{END}} \left| u_k - u_k^{ref} \right| dz + \int_0^{z_{END}} \left| v_k - v_k^{ref} \right| dz \right) \tag{13}$$

where f_m and f_m^{ref} are model predicted and reference values of natural frequencies, u_k, v_k and u_k^{ref}, v_k^{ref} are predicted and reference displacement components (integrals are evaluated approximately by trapezoidal rule), q is a weight coefficient, and N_f and N_d are numbers of used frequencies and displacements, respectively. Good results were obtained for $N_f = 5$, $N_d = 4$, $q = 15$.

Table 5. Segment data.

N_{seg}	1	2	3	4	5	6
$\log EI_x$	22.7105	19.8247	18.5612	16.9871	15.9708	15.7200
EI_x	7.2953×10^9	4.0715×10^8	1.1509×10^8	2.3845×10^7	8.6304×10^6	6.7160×10^6
$\log EI_y$	23.3283	22.4936	21.3745	20.2470	19.4379	18.9420
EI_y	1.3532×10^{10}	5.8728×10^9	1.9179×10^9	6.2110×10^8	2.7655×10^8	1.6842×10^8

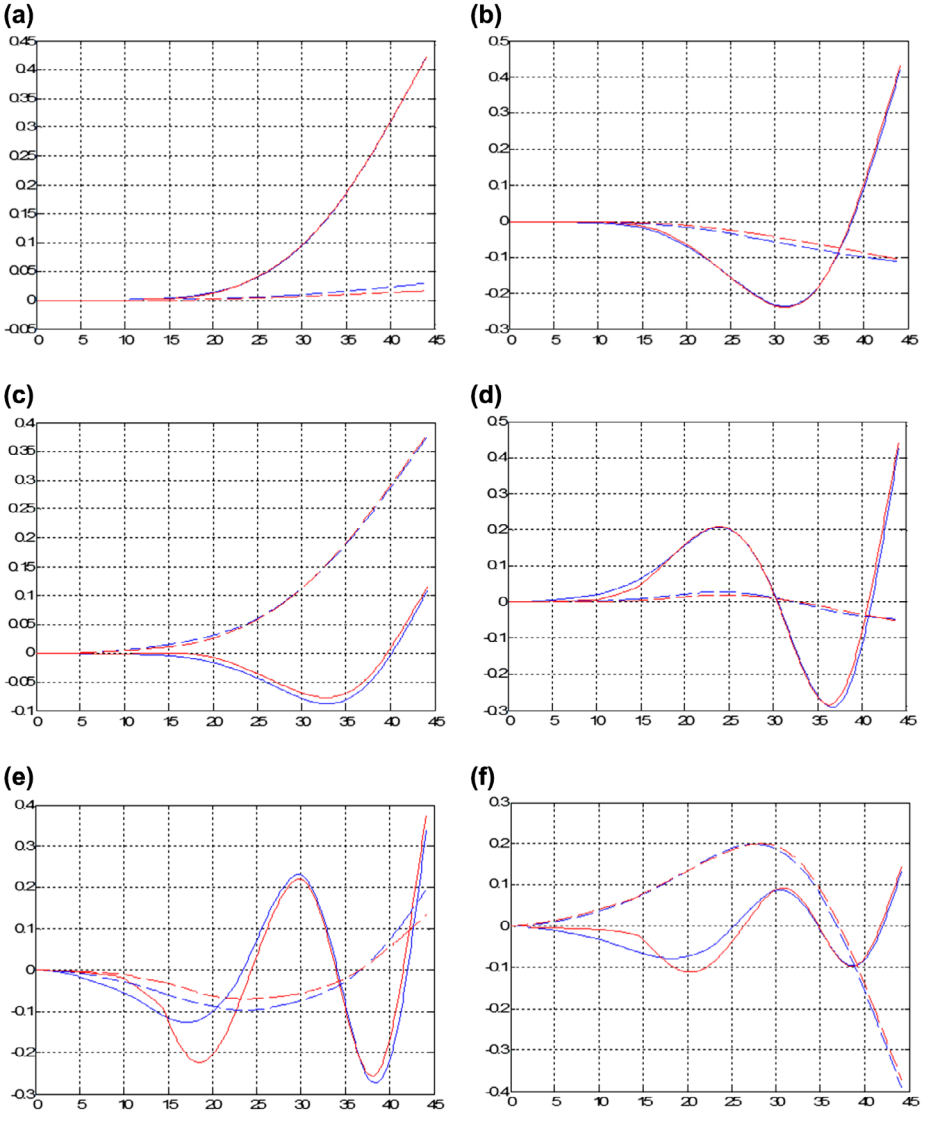

Figure 5. Identified (blue) and FEM computed (red) modal displacements in flap (solid lines) and lead-lag (dashed lines) directions for the six-segment simplified beam-mass blade model for six lowest modes (a)–(f).

The results of identification analyses with given parameters for the objective function are shown below. Here, identified values of logarithms of bending

Table 6. Segment data.

N_{seg}	1	2	3	4	5
$\log EI_x$	22.6188	19.9943	18.4494	18.2133	17.114
EI_x	6.6561×10^9	4.8241×10^8	1.0291×10^8	8.1271×10^7	2.7072×10^7
$\log EI_y$	23.4251	22.1001	21.832	21.2535	20.0834
EI_y	1.4907×10^{10}	3.9623×10^9	3.0305×10^9	1.6993×10^9	5.2736×10^8
N_{seg}	6	7	8	9	10
$\log EI_x$	16.7606	15.9663	15.6166	15.2014	15.1873
EI_x	1.9012×10^7	8.5916×10^6	6.0562×10^6	3.9984×10^6	3.9424×10^6
$\log EI_y$	19.928	19.5295	18.9319	18.8288	18.6508
EI_y	4.5146×10^8	3.0308×10^8	1.6673×10^8	1.5040×10^8	1.2588×10^8

stiffnesses and corresponding values of bending stiffnesses are presented in Table 5.

Respectively, the obtained minimal value of the objective function is $F_{\min} = 3.0868$.

In Figure 5 identified modal shapes are shown with blue lines, and actual modes provided by ABAQUS, are depicted with red ones. Solid and dashed lines correspond to the flap bending and lead-lag vibrations, respectively. As one can see very close agreement has been obtained using the reduced model.

The next experiment was carried out to test opportunities of improvement on the quality of identification by increasing the order of the model. For this we divided segment from 3 to 5 used in the previous model into two parts again, thus the model with ten segments was obtained. So in this case, lumped masses m_k have values:

$$[6985.084, 1765.386, 476.462, 416.973, 357.483, 271.076, 213.435, 197.095, 180.755, 84.931],$$

and twisting angles α_k are as follows

$$[-12.856, -10.263, -7.0025, -5.6675, -4.3325, -2.9975, -2.195, -1.925, -1.655, -1.385].$$

The results of identification are given below in Table 6. First of all, we see good stability of identification results and better accuracy: achieved value of the objective function $F_{\min} = 1.6713$ is nearly half the previous case, so graphs in Figure 6 demonstrate this.

It is worth mentioning that the procedure developed provides good identification of lower vibrational modes and frequencies for a real rotor blade taking account of the coupling between flap and lead-lag motions caused by blade twisting even within the framework of classical Euler–Bernoulli beam model.

5. Conclusions

In this present paper, a modified approach to construction of a beam-type simplified dynamic model of an HAWT composite blade is proposed. The model is based on an identification procedure using modal data attained by detailed FEM simulations.

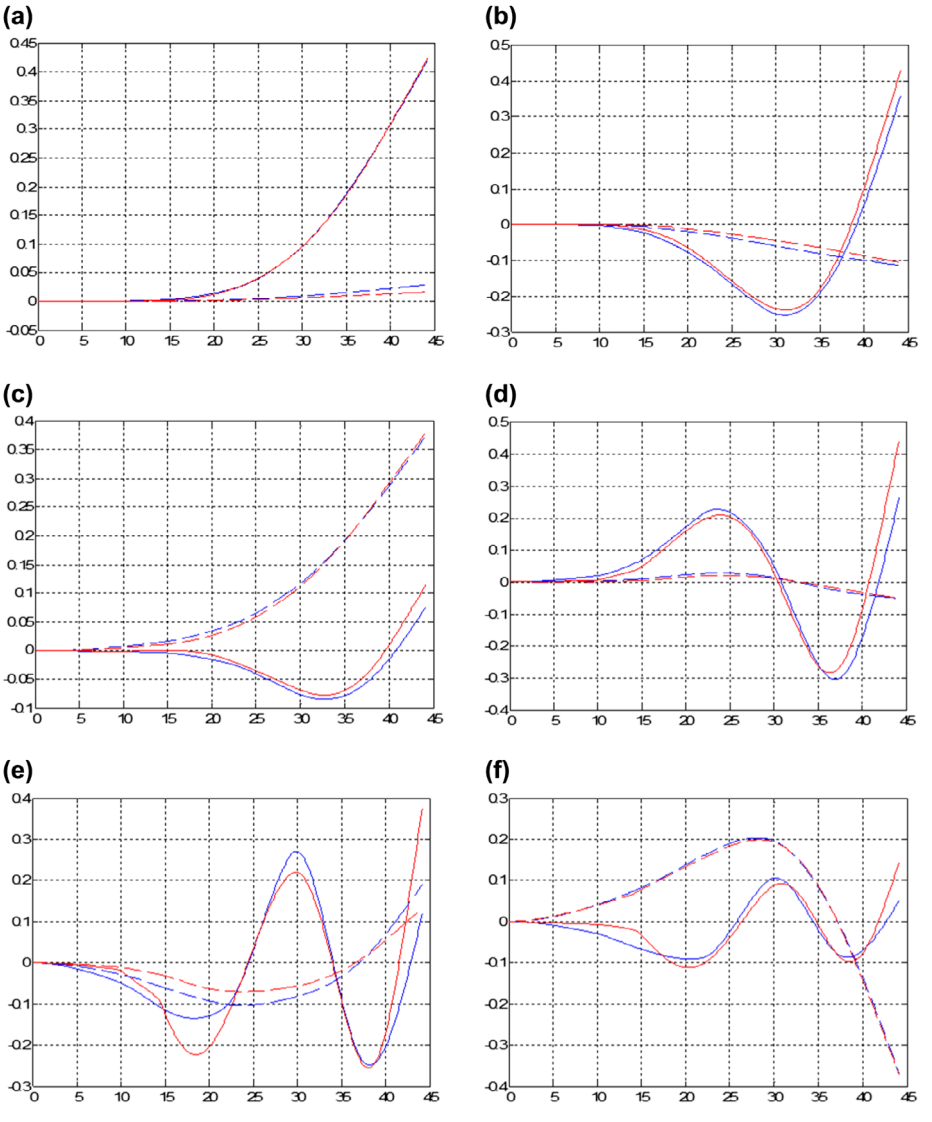

Figure 6. Identified (blue) and FEM computed (red) modal displacements in flap (solid lines) and lead-lag (dashed ones) directions for the 10-segment simplified beam-mass blade model for six lowest modes (a)–(f).

The constructed beam-type mathematical model takes into account structural pre-twisting of the blade along its length that does not allow splitting flap and lead-lag motions. Therefore, it allows interaction between different modes of vibration.

An objective function is defined which describes a measure of absolute differences between results of modal simulations obtained by the proposed simplified model and the detailed FEM ones. The results of numerical experiments carried out show that better identification results are obtained when in the objective function the modular norms are used instead of quadratic norms. Additional

positive effect is obtained using logarithmic scaling of identifiable bending stiffness parameters.

The identification procedure is carried out using the global minimisation algorithm 'DIRECT' with constraints imposed based on a priori information (solution on the compact) which provided stable solution results for the ill-posed inverse problem. The results of the identified beam-type models with different number of beam and mass sections are in agreement with the reference FEM simulation data both qualitatively and quantitatively.

It is conjectured that further improvements can be achieved using more complex simplified models with distributed masses and inhomogeneous section stiffness distribution. Any such enhanced model will need to use an underlying mechanics principle such as minimum potential energy along with a consistent or inconsistent finite element formulation for approximation of displacement and possibly stress fields subsequent to segmentation and discretisation.

Acknowledgements

The authors wish to express their gratitude for the financial support provided by TurkAz Enerji Ltd.

Disclosure statement

No potential conflict of interest was reported by the authors.

Funding

This work was supported by TurkAz Enerji Ltd. [contract number AESZ P56658].

ORCID

A. S. Fallah http://orcid.org/0000-0002-0382-633X

References

ABAQUS. (2014). v. 6.14 User Guide.

Bakushinsky, A., & Goncharsky, A. (1994). *Ill-posed problems: Theory and applications*. Dordrecht: Springer Science+Business Media.

Baruch, M. (1997). Modal data are insufficient for identification of both mass and stiffness matrices. *AIAA Journal, 35*(11), 1797–1798.

Chen, K.-N., & Chen, P.-Y. (2010). Structural optimization of 3 MW wind turbine blades using a two-step procedure. *International Journal for Simulation and Multidisciplinary Design Optimization, 4*, 159–165.

DIRECT. (2003). Optimization algorithm user guide. Retrieved from http://www4.ncsu.edu/~ctk/Finkel_Direct/

Gruber, M. H. J. (2014). *Matrix algebra for linear models*. San Francisco, CA: Wiley.

Lee, U. (1995). Equivalent dynamic beam–rod models of aircraft wing structures. *Aeronautical Journal, 99*(990), 450–457.

Serrano-González, J., & Lacal-Arántegui, R. (2016). Technological evolution of onshore wind turbines – A market-based analysis. *Wind Energy,* 19, 2171–2187. Retrieved from http://onlinelibrary.wiley.com/doi/10.1002/we.1974/full

Staino, A., & Basu, B. (2015). Emerging trends in vibration control of wind turbines: A focus n a dual control strategy. *Philosophical Transactions of the Royal Society A, 373*, 20140069. Retrieved from http://rsta.royalsocietypublishing.org/content/373/2035/20140069, http://rsta.royalsocietypublishing.org/content/roypta/373/2035/20140069.full.pdf

Trivailo, P. M., Dulikravich, G. S., Sgarioto, D., & Gilbert, T. (2006). Inverse problem of aircraft structural parameter estimation: Application of neural networks. *Inverse Problems in Science and Engineering, 14*(4), 351–363.

Wiser, R. H., & Bolinger, M. (2015). *Wind technologies market report*. U.S. Department of Energy, 2016. Retrieved from https://emp.lbl.gov/publications/2015-wind-technologies-market-report